OPEN ACCESS
IOP Publishing
Environmental Research Letters
Environ. Res. Lett. 9 (2014) 104018 (8pp)
doi:10.1088/1748-9326/9/10/104018

The days of plenty might soon be over in glacierized Central Asian catchments

Annina Sorg[1,2], Matthias Huss[3], Mario Rohrer[4] and Markus Stoffel[1,2]

[1] Institute for Environmental Sciences (ISE), University of Geneva, Route de Drize 7, 1227 Carouge, Switzerland
[2] dendrolab.ch, Institute of Geological Sciences, University of Berne, Baltzerstrasse 1+3, 3000 Bern, Switzerland
[3] Department of Geosciences, University of Fribourg, 1700 Fribourg, Switzerland
[4] Meteodat GmbH, Technoparkstrasse 1, 8005 Zurich, Switzerland

E-mail: annina.sorg@dendrolab.ch

Received 20 July 2014, revised 4 September 2014
Accepted for publication 18 September 2014
Published 20 October 2014

Abstract

Despite the fact that the fast-growing population of Central Asia strongly depends on glacial melt water for fresh water supply, irrigation and hydropower production, the impact of glacier shrinkage on water availability remains poorly understood. With an annual area loss of 0.36 to 0.76%, glaciers are retreating particularly fast in the northern Tien Shan, thus causing concern about future water security in the densely populated regions of Bishkek and Almaty. Here, we use exceptionally long in-situ data series to run and calibrate a distributed glacio-hydrological model, which we then force with downscaled data from phase five of the Climate Model Intercomparison Project CMIP5. We observe that even in the most glacier-friendly scenario, glaciers will lose up to two thirds (−60%) of their 1955 extent by the end of the 21st century. The range of climate scenarios translates into different changes in overall water availability, from *peak water* being reached in the 2020s over a gradual decrease to *status quo* until the end of the 21st century. The days of plenty, however, will not last much longer, as summer runoff is projected to decrease, independent of scenario uncertainty. These results highlight the need for immediate planning of mitigation measures in the agricultural and energy sectors to assure long-term water security in the densely populated forelands of the Tien Shan.

S Online supplementary data available from stacks.iop.org/ERL/9/104018/mmedia

Keywords: climate change, glacier retreat, hydrology, water resources, Tien Shan

(Some figures may appear in colour only in the online journal)

1. Introduction

As future summers are expected to become drier and hotter, the buffering capacity of glaciers will become more important for Central Asia's fresh water supply, irrigation, and hydropower potential (Barnett *et al* 2005). However, the glacio-hydrological system of the region is currently undergoing a substantial change, as increased runoff from glacier wasting will eventually result in decreasing melt water amounts from strongly reduced glacier volume and area. A crossing of this tipping point (*peak water*) is expected to occur earlier in northern Tien Shan (Vilesov and Uvarov 2001, Kotlyakov and Severskiy 2009) than in the higher inner and eastern Tien Shan ranges (Hagg *et al* 2013b, Ye *et al* 2005), but studies using sophisticated distributed glacio-hydrological models and state-of-the-art climate projections are still rare (Lutz *et al* 2013, Zhang *et al* 2007, Hagg *et al* 2013a).

In this study, we assess past and future glacier- and runoff changes with the distributed Glacier Evolution Runoff

Content from this work may be used under the terms of the Creative Commons Attribution 3.0 licence. Any further distribution of this work must maintain attribution to the author(s) and the title of the work, journal citation and DOI.

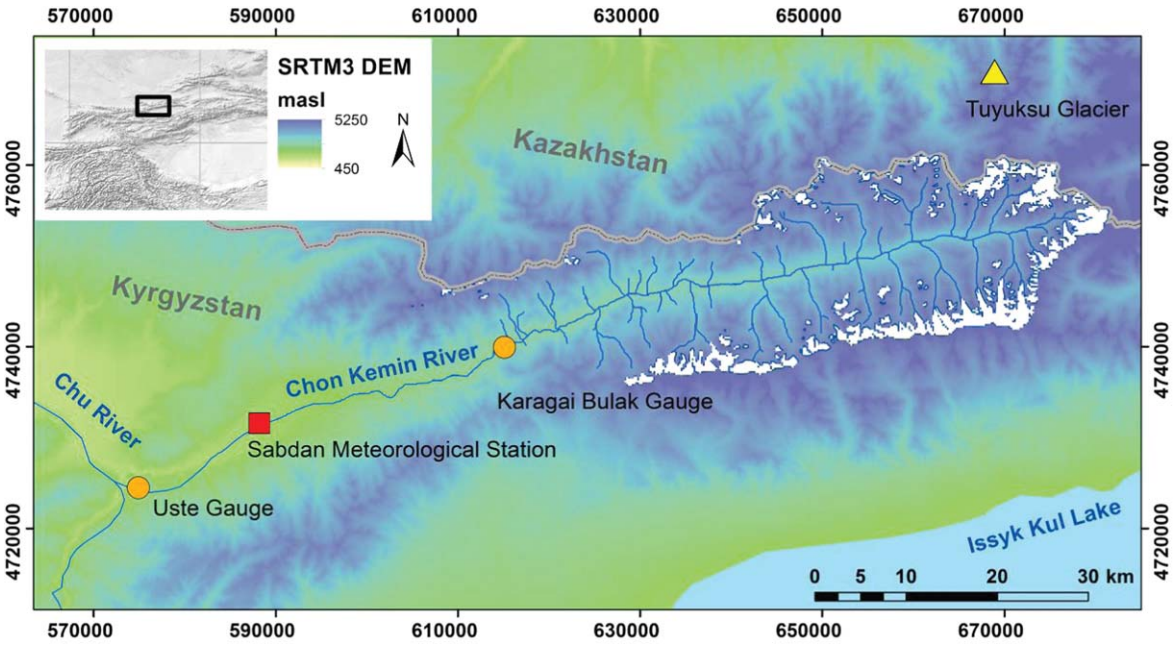

Figure 1. Overview of the glacierized Chon Kemin catchment in the Kyrgyz-Kazakh border region.

Model GERM (Huss *et al* 2008). In a novel approach, we combine several observational time series covering large parts of the 20th century with satellite-derived snow cover data to calibrate and validate all relevant processes in the glacio-hydrological model. Although the Tien Shan mountains are generally referred to as a data-sparse region (Lutz *et al* 2013, Unger-Shayesteh *et al* 2013), we rely here on exceptionally long data series of temperature and precipitation (1937–90), discharge (1951–98) and annual glacier mass balance and Equilibrium Line Altitudes (ELA 1957-today). We also included annual snow cover duration from the Advanced Very High Resolution Radiometer (AVHRR 1985–89) and daily snow coverage from Landsat scenes (1977/1979) as well as information on high-altitude precipitation and basin evaporation (Aizen *et al* 2007) to calibrate all relevant parameters and processes.

Unprecedented for Central Asia, we then force the model with downscaled data from phase five of the Climate Model Intercomparison Project CMIP5 (Taylor *et al* 2012) to close the meteorological data gap of the past 20 years since the collapse of the Soviet Union and to make scenario-based glacier and runoff projections in the unregulated Chon Kemin catchment up to the end of the 21st century.

2. Study area

The deeply incised Chon Kemin valley (figure 1) is located in the Kyrgyz part of the Tien Shan mountains, between the Zailiyskiy and Kungey Alatau ranges at the border to Kazakhstan. Running over 120 km from west to east, the valley stretches from 1500 m above sea level to Chok Tal peak at 4760 m asl, with an average elevation of 3170 m asl. The headwater catchment above Karagai Bulak gauge (42.8° N, 76.41°E) covers an area of 1037 km^2, of which around 11% (112 km^2) have been covered by 217 glaciers in 1999 (Bolch 2007). Eastern and Western Aksu are the largest glaciers in the valley, covering 6.65 and 5.52 km^2, respectively.

The Chon Kemin river is the most important tributary (40% of total runoff) to the Chu river (Katchaganov 2011), providing Kyrgyzstan's capital Bishkek with fresh water before running further northwest to the Kazakh steppe. During summer, the Chon Kemin river is fed mostly by melt water from glaciers.

The Zailiyskiy Alatau constitutes the first montane barrier for northern and western air masses travelling from Siberia and the Kazakh steppes to Central Asia (Aizen *et al* 1997, Bolch 2007). Due to its west-east-orientation with high mountains at the valley end, the Chon Kemin valley is predominantly influenced by air masses coming from west (Katchaganov 2011). Mean annual air temperature at Sabdan station (42.70°N, 76.10°E) is 4.9 °C and mean annual precipitation is 445 mm (mean 1937–98). Precipitation minima occur in winter as a result of the Siberian anticyclone, whereas most precipitation falls in early summer due to cyclonic activity and convective precipitation (Böhner 1996).

3. Data, models and methods

3.1. Glacio-hydrological model

For this study, we use the fully distributed, deterministic, conceptual glacio-hydrological Glacier Evolution Runoff Model (GERM) (Huss *et al* 2008). The model calculates all components of the surface water balance with a focus on accumulation and melt processes on glaciers, and runs at high spatial and temporal resolutions (200 meters and one day,

respectively). While requiring a minimum of input data, the model includes transient glacier changes, which is particularly important when glaciers are not in balance with the prevailing climate (Huss *et al* 2008). Ice thickness distribution for each individual glacier in the catchment as well as overall glacier volumes are derived from an inversion of surface topography based on the principles of ice flow dynamics (Huss and Farinotti 2012). Transient changes in 3D glacier surface geometry and ice volume are assessed with the empirical, mass conserving Δh-parameterization (Huss *et al* 2010). This function approximates glacier surface elevation changes in response to surface mass balance forcing as given by ice flow dynamics. By intersecting calculated elevation changes with local glacier bed elevation, glacier area change in the spatial domain is obtained. Glacier mass balance, basin evaporation and runoff are calculated in daily time-steps.

We use a simplified energy-balance approach (Oerlemans 2001), which outperforms temperature-index-methods for long modeling periods and in continental climates as it is less sensitive to temperature changes (Oerlemans 2001, Pellicciotti *et al* 2005). This renders the simplified energy balance approach particularly adequate for modeling in arid regions like Central Asia and over multi-decadal time periods with significant trends in air temperature. The energy available for melt is calculated as

$$\psi = \{a(1-\alpha)Q_E\} + \{c_0 + c_1 T\}, \quad (1)$$

where a is the atmospheric transmission to solar irradiance (reduced incoming shortwave radiation due to cloudiness or haze), α the surface albedo for snow, ice or firn, and Q_E the clear-sky shortwave radiation (mean daily potential global radiation calculated from slope, aspect and topographic shading) representing the short-wave radiation balance. The sum of the long-wave radiation balance and turbulent heat exchanges is parameterized using the parameters c_0, c_1 (set to 10 W m^{-2}K^{-1}, according to Oerlemans (2001)), and air temperature T.

An empirical evaporation model is implemented in GERM, which calculates daily potential evaporation based on air temperature and the saturation vapor pressure (Huss *et al* 2008, Hamon 1961). The model considers five surface types (snow, ice, rock, low vegetation and forest) and has an interception reservoir. Potential evaporation is reduced to actual evaporation for each surface type using a factor that includes a function accounting for the decrease of soil moisture.

The water available for runoff is determined daily at every grid cell by solving the water balance using the calculated quantities for liquid precipitation, melt and evaporation (Huss *et al* 2008). The runoff routing model is based on the concept of linear storage, with an interception-, slow- and fast reservoir (Farinotti *et al* 2012, Huss *et al* 2008).

3.2. Multi-variable calibration and validation

We developed a new multi-variable calibration and validation approach combining several observational time series that cover large parts of the 20th century with satellite-derived snow cover data to calibrate all relevant processes in the glacio-hydrological model. It has been shown that parameters of glacier melt models can be subject to long-term variations (Huss *et al* 2009). To obtain a robust parameter set for application over the next century, we used the longest possible period for parameter determination and therefore did not split the datasets, which would be important if only one variable (e.g. discharge) were used to constrain model parameters. Here, we rely on a suite of different observational variables and can thus use some datasets for calibration (i.e. glacier mass balance, snow cover evolution, equilibrium line altitudes) and others for independent validation (i.e. discharge, glacier area change). This approach allows a realistic reproduction of all runoff components, which reduces the problem of equifinality ('right answers for wrong reasons'; (Hagg *et al* 2013a).

The model has been manually calibrated and validated to determine the key model parameters. In a first step, parameters describing the spatial distribution of meteorological variables were constrained based on values from a previous study (Aizen *et al* 2007) to reach a realistic level of mean annual runoff. Then, the melt parameters were calibrated to accomplish a reasonable agreement with observed accumulation and ablation processes of snow and ice. Last, the runoff routing parameters were tuned to optimize the seasonally realistic distribution of runoff as indicated by the field data series.

3.3. Input and calibration data

We rely here on exceptionally long data series of temperature and precipitation (1937–90), discharge (1951–98) and annual glacier mass balance and ELA (1957–today) for forcing and calibrating the model. We also included annual snow cover duration from the Advanced Very High Resolution Radiometer (AVHRR 1985–89) and daily snow coverage from Landsat scenes (1977/1979) as well as information on high-altitude precipitation and basin evaporation (Aizen *et al* 2007) to calibrate all relevant parameters and processes (supplementary figures S1, S4–S7 and supplementary tables S1–S3 available at stacks.iop.org/ERL/9/104018/mmedia).

Temperature and precipitation time series from Sabdan meteorological station (1524 m asl) were available in daily resolution for the time period 1937–90 from the Royal Netherlands Meteorological Institute. The precipitation data series contained gaps, which we filled with daily data from the National Climatic Data Center (NOAA). Discharge data from Karagai Bulak gauge (2078 m asl) were available in daily resolution for the time period 1951–96 (Kirgizgidromet 1936–2002). Mass balance and ELA have been assessed since 1957 at Tuyuksu glacier, which makes them the longest series in Central Asia (WGMS 2009). Glacier outlines are from Bolch (2007), who mapped the glacier coverage in the Chon Kemin and surrounding valleys using a snow-free Landsat ETM+ scene from 08/08/1999. We have also digitized glacier outlines reflecting the situation in the 1950s based on topographic maps at the scale of 1:100 000 (Soviet Topographic Map 1988) to calibrate the

model. Land use classification has been derived from a supervised classification of the same Landsat ETM+ scene as used for the glacier outlines (08/08/1999). Snow cover has been used for visual comparison from four Landsat scenes in 1977 (17/04, 23/05, 07/09 and 01/11) and two Landsat scenes in 1979 (30/03 and 12/05). Annual snow cover duration has been assessed from the Advanced Very High Resolution Radiometer (AVHRR) at a resolution of 1 km starting in 1986 (Dietz *et al* 2013). The digital elevation model (DEM) and catchment area delineation are based on data from the Shuttle Radar Topography Mission SRTM3 (Jarvis *et al* 2008).

3.4. Downscaling of future climate data

The calibrated model was then forced with daily time series of future temperature and precipitation. To cover the whole range of possible 21st century climatic changes in the glacio-hydrological modeling (Vuuren *et al* 2011), we evaluated all available Global Circulation Model (GCM) runs for the two most extreme Representative Concentration Pathways scenarios (Meinshausen *et al* 2011), RCPs 2.6 and 8.5, which have been generated under the CMIP5 (Taylor *et al* 2012). Similar to previous studies (Lutz *et al* 2013, Immerzeel *et al* 2013), we selected the four GCM runs spanning the 10th and 90th percentiles of changes in summer temperature and in total precipitation and downscaled these four scenarios with the delta-change approach (Prudhomme *et al* 2002) to obtain transient daily time series of temperature and precipitation until 2099 with the same resolution, characteristics and variance as the station data. This procedure intentionally suppresses some of the year-to-year variability observed in the past in order to reveal interpretable long-term trends in the output variables. All modeling results span the range of the four possible future scenarios (dry-cold, dry-warm, wet-cold and wet-warm future climates) and are compiled for the past (1955–99), the present and near future (2000–49) and the far future (2050–99).

3.5. Statistical trend analysis of past temperature, precipitation and runoff

Trends in measured temperature, precipitation, mass balance and runoff were analyzed with the 2-sided non-parametric Mann-Kendall test at the 80, 90 and 95% significance levels (Kendall 1975, Helsel and Hirsch 1992). Serial correlation was removed using Sen's slope method (Sen 1968) and a pre-whitening approach (Zhang *et al* 2000). With the help of moving time windows, the multiple trend tests were computed for all time windows of at least 30 years in length during the common 1937–90 period. Two matrices were compiled for each parameter: trends are indicated with the standardized test statistics τ, trend significance is indicated by the 2-sided p-value.

4. Results

4.1. Observed changes in climate and runoff

Like in other parts of Central Asia, mean annual air temperature (MAAT 1937–98: 4.9 °C) and mean annual precipitation (MAP 1937–98: 445 mm) have increased in the Chon Kemin valley over recent decades (Sabdan meteorological station, 1524 m asl; supplementary figure S2), probably as a result of the weakening of the Siberian anticyclone (Giese *et al* 2007). Runoff at Uste gauge in the Chon Kemin valley has also increased significantly during the same period. Increasing spring temperatures have likely caused enhanced snow melt and thus significant increases in spring discharge. Temperature and runoff have also significantly increased in summer and fall, thus indicating enhanced glacier melting and a prolongation of the melting period (Kriegel *et al* 2013, Bolch 2007).

4.2. Projected changes in climate, glaciers and runoff

MAAT and MAP are likely to increase further by +1.6 to +7.8 °C and −2 to +20%, respectively, according to the four GCM runs spanning the range of dry-cold, dry-warm, wet-cold and wet-warm future CMIP5 climates (2081–99 versus 1961–90; supplementary figure S3).

These changes in climate are projected to result in negative glacier mass balances and to cause a rise in ELA from 3922 (average 1955–99) to 3976–4031 (2000–49) and 3991–4409 (2050–99) m asl, depending on the scenario, and thus cause significant losses in glacier area and volume. In the more 'glacier-friendly', dry-cold and wet-cold scenarios, glaciers are projected to cover 38 and 53 km^2 by 2099, thus representing 29 and 40% of their extent in 1955, respectively. In the more pessimistic, dry-warm and wet-warm scenarios, glaciers in the Chon Kemin basin are expected to disappear completely around 2080 (figures 2(a), (b), table 1). These distinct differences between the cold and warm scenarios confirm that enhanced glacier shrinkage is strongly correlated with increasing air temperatures in the Tien Shan (Lutz *et al* 2013, Ye *et al* 2005, Kriegel *et al* 2013).

The projected depletion of glacial reserves translates into three different response types of glacial- and total runoff (figure 2(c), table 1): According to the warm scenarios, releases from annual glacier storage change can be expected to culminate in the 2020s, with a subsequent drop in glacial and total runoff. The dry-cold scenario leads to a gradual decrease in total runoff, despite fairly constant glacial runoff over the entire 21st century. The most glacier-friendly, wet-cold scenario results in almost no changes in glacial and total runoff until 2099. The timing of peak water in the warm scenarios is in line with a previous study (Mamatkanov *et al* 2006), whereas results from the cold scenarios correspond more with comparable studies for higher altitude catchments in Central Asia (Hagg *et al* 2013a) and the Himalayas (Immerzeel *et al* 2013, Lutz *et al* 2014).

These fundamental changes in the headwater catchment will ultimately influence seasonal runoff in the Chon Kemin

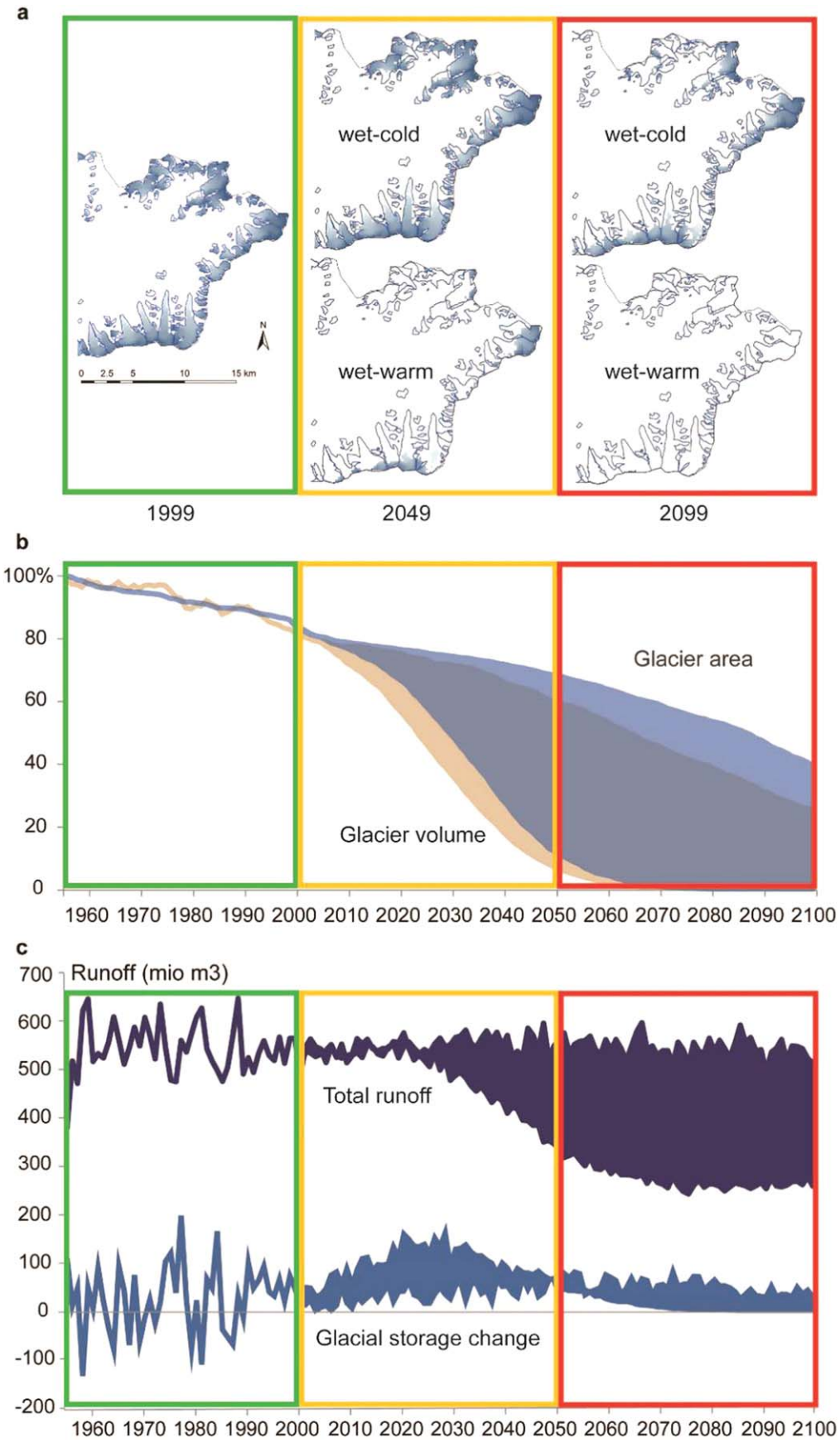
a
wet-cold
wet-warm
wet-cold
wet-warm
N
0 2.5 5 10 15 km
1999
2049
2099
b
100%
80
60
40
20
0
Glacier area
Glacier volume
1960 1970 1980 1990 2000 2010 2020 2030 2040 2050 2060 2070 2080 2090 2100
c
Runoff (mio m3)
700
600
500
400
300
200
100
0
-100
-200
Total runoff
Glacial storage change
1960 1970 1980 1990 2000 2010 2020 2030 2040 2050 2060 2070 2080 2090 2100

Figure 2. Glacier and runoff evolution in the Chon Kemin catchment in the past (1955–99; green), the present and near future (2000–49; orange) and the far future (2050–99; red): (a) Changes in glacier extent at the end of each period (outlines are from 1955). (b) Glacier area and ice volume evolution relative to 1955. (c) Total basin runoff and annual glacier storage change (negative in years with positive mass balance, positive in years with glacier mass loss).

Table 1. Percental changes in glacio-hydrological key parameters for all scenarios (dry-warm, wet-cold, wet-warm, dry-cold) relative to the past (1955–99).

All numbers are in percent	Present and near future (2000–49)				Far future (2050–99)			
Scenario	Dw	Wc	Ww	Dc	Dw	Wc	Ww	Dc
Glacier area	−40	−19	−43	−19	−97	−41	−98	−48
Glacier volume	−49	−23	−52	−24	−98	−56	−99	−64
Glacier storage change	+275	+17	+288	+36	−54	+62	−67	+93
Precipitation	0	+5	+7	+1	−1	+15	+17	−1
Evaporation	+15	+8	+22	+4	+25	+21	+46	+9
Total runoff	−19	−1	−6	−4	−49	0	−37	−13
Total summer runoff	−15	−4	−13	−9	−66	−9	−61	−22
Snow cover duration	−2	+5	−5	+5	−21	−1	−29	−2

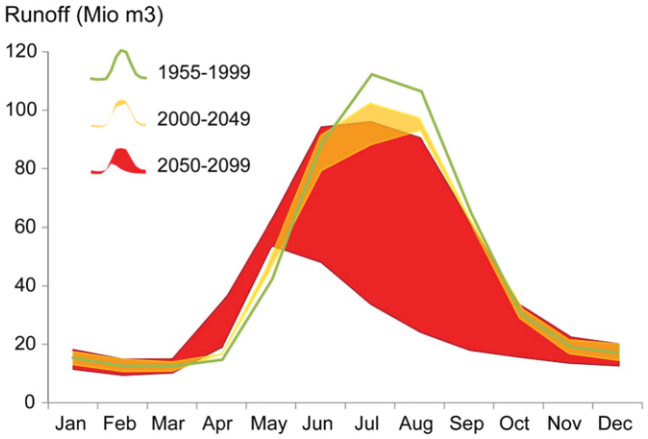

Figure 3. Averaged monthly runoff distribution of the Chon Kemin River in the past (1955–99), the present/near future (2000–49) and the far future (2050–99) including all simulated scenarios.

river (figure 3)—as in other catchments in the same region (Hagg *et al* 2007)—with potentially immense repercussions on agriculture and fresh water supply in the Bishkek area. Summer runoff (JJA) in the Chon Kemin River is projected to decrease by –4 to –15% (2000–49), before reaching a total reduction of –9 to –66% (2050–99) as compared to the past (1955–99). Winter runoff is likely to decrease for the warm scenarios and to increase for the cold scenarios. Although all scenarios predict increasing winter precipitation, air temperatures are still cool enough so that most winter precipitation is snow at high elevation. The slight decrease in winter runoff for the warm scenarios is attributed to the stronger depletion of the groundwater storage during the much drier previous summer season. In spring (MAM), increasing runoff amounts are projected for both the near and the far future (+7 to +23% and +18 to +62%, respectively, depending on the scenario). This increase is reflective of more winter precipitation and enhanced snowmelt in spring. Hence, average annual snow cover duration is projected to decrease from 153 d (1955–99) to 108–151 d (2050–99), after having fluctuated between 145–161 d (2000–49).

As a result of higher air temperatures, mean annual actual evaporation is projected to increase from 384 (past) to 405–96 and further up to 433–622 mm a^{-1} (averages 2000–49 and 2050–99, respectively), which is comparable to other studies carried out in the region (Vilesov and Uvarov 2001, Aizen *et al* 2007). The losses due to evaporation are thus becoming more important and will exacerbate the situation of reduced melt water availability.

5. Discussion

Uncertainties occur at all stages of glacier and runoff modeling, and may stem from various sources (Huss *et al* 2014). We discuss here the influence of measured input and calibration data, the parameterization of the glacio-hydrological model, climate models and the downscaling procedure, as well as feedback mechanisms.

The errors in measured data are likely to be rather small, as all data series were systematically checked for inhomogenities. Moreover, the multi-variable calibration implemented in GERM keeps the impact of single data sets limited. Whereas the current glacier extent has been assessed with high precision, past glacier extent used for the initialization of the model calibration might possibly be slightly overestimated due to misinterpreted snow cover on some aerial photographs used for the 1950s topographic maps (Sorg *et al* 2012). Simulation and calibration of daily and annual snow cover highly depend on the applied threshold of perceptible snow water equivalents on the satellite images, which were constrained based on literature (Gafurov *et al* 2012).

Uncertainties also arise from the glacio-hydrological model. Although the model is fully distributed at a high spatial resolution, an even higher resolution could improve the results—at the costs of an exponential increase of computation time. Also, the simulation of surface elevation changes for short-term advance phases is expected to be

uncertain, but this drawback has a minor influence on the results of this study as few years with glacier mass gain were observed. Other enhancements could include the use of climate data from high altitude meteorological stations, although they are located in neighboring valleys and are thus subject to differing meteorological patterns. Calibration would certainly also benefit from more ground truthing in the catchment (e.g. mass balance, radio echo soundings of the ice thickness, seasonal precipitation gradients), but acquiring such data is laborious and could only cover short periods. As an alternative, simulated glacier volume change could be constrained with regional volume changes from GRACE (Gravity Recovery and Climate Experiment) or by comparison of repeat high-resolution DEMs. At the bottom line, however, the energy-balance-based melt model and the calibration covering a multitude of very long data-series strongly reduce the issue of equifinality and strengthen the consistency of parameters over long time periods.

Structural differences among the GCMs, by contrast, are an important source of uncertainty, as models respond differently to the same external forcing (Hawkins and Sutton 2009). In the past, uncertainty contribution from climate models has shown to outweigh the uncertainty stemming from glacier models (Gosling *et al* 2011) or to be comparable (Lutz *et al* 2013). We therefore attempted to further limit climate model uncertainty through a representative selection of RCPs and GCMs spanning the full range of possible future climates. The selection was based on summer temperature and annual precipitation, both representing the key drivers of glacier mass balance.

Another important source of uncertainty are future changes in evaporation, for which both the direction and magnitude are highly debated (Barnett *et al* 2005). Our projected changes in evaporation are in line with another study for this region (Aizen *et al* 2007), but it would certainly be most helpful to have more informed data on future evaporation in Central Asia.

6. Conclusion

Irrespective of scenario uncertainty, our study clearly points to significant glacier wasting until the end of the 21st century, which will translate into reduced water availability during summer. Glaciers in the Chon Kemin valley—and in many comparable catchments in Northern Tien Shan—may disappear completely by the end of the 21st century in a worst-case-scenario. Even in the most glacier-friendly scenario, glaciers will lose up to two thirds (−60%) of their 1955 extent by the end of the 21st century. The range of climate scenarios translates into different changes in overall water availability, from *peak water* being reached in the 2020s over a gradual decrease to *status quo* until the end of the 21st century. The days of plenty, however, will not last much longer, as summer runoff is projected to decrease, independent of scenario uncertainty. These results highlight the need for immediate planning of flexible mitigation measures in the agricultural and energy sectors to avoid an exacerbation of inter-state conflicts and to assure long-term water security for the Bishkek capital region, where more than a million people live. On the water supply side, existing dams and backup-reservoirs further downstream could partly take over the role of glaciers as intra- and inter-annual buffers in the hydrological cycle (Sorg *et al* 2014). On the water demand side, a shift to less water-intensive crops and the restoration of the often outdated irrigation channels could reduce water demand during summer. Although the Soviet legacy and the current political context complicate such approaches in Central Asia, transboundary collaboration projects like the Chu Talas basin agreement are encouraging steps towards a reasonable water allocation in a changing future.

Acknowledgements

We thank T Bolch, C Corona and A Dietz for providing data and for technical assistance. This study was supported by the ACQWA project (Framework Program 7 of the European Commission under Grant Nr. 212250; www.acqwa.ch). W Hagg and an anonymous reviewer are thanked for helpful comments on the manuscript.

References

Aizen V B, Aizen E M and Kuzmichenok V A 2007 Geo-informational simulation of possible changes in Central Asian water resources *Glob. Planet. Change* **56** 341–58

Aizen V B, Aizen E M, Melack J M and Dozier J 1997 Climatic and hydrologic changes in the Tien Shan, Central Asia *J. Climate.* **10** 1393–404

Barnett T P, Adam J C and Lettenmaier D P 2005 Potential impacts of a warming climate on water availability in snow-dominated regions *Nature* **438** 303–9

Böhner J 1996 Secular climate fluctuatians and recent climate trends in Central and High Asia (in German) *Göttinger Geographische Abhandlungen* 101

Bolch T 2007 Climate change and glacier retreat in northern Tien Shan (Kazakhstan/Kyrgyzstan) using remote sensing data *Glob. Planet. Change* **56** 1–12

Dietz A, Kuenzer C, Conrad C and Dech S 2013 Changes of snow cover characteristics in Central Asia between 1986 and 2012 derived from AVHRR and MODIS time series *Eastern Snow Conf. (Huntsville, Ontario, Canada)*

Farinotti D, Usselmann S, Huss M, Bauder A and Funk M 2012 Runoff evolution in the Swiss Alps: projections for selected high-alpine catchments based on ENSEMBLES scenarios *Hydrol. Process.* **26** 1909–24

Gafurov A, Kriegel D, Vorogushyn S and Merz B 2012 Evaluation of remotely sensed snow cover product in Central Asia *Hydrol. Res.* **44** 506–22

Giese E, Mossig I, Rybski D and Bunde A 2007 Long-term analysis of air temperature trends in Central Asia *Erdkunde* **61** 186–202

Gosling S N, Taylor R G, Arnell N W and Todd M C 2011 A comparative analysis of projected impacts of climate change on river runoff from global and catchment-scale hydrological models *Hydrol. Earth Syst. Sci.* **15** 279–94

Hagg W, Braun L N, Kuhn M and Nesgaard T I 2007 Modelling of hydrological response to climate change in glacierized Central Asian catchments *J. Hydrol.* **332** 40–53

Hagg W, Hoelzle M, Wagner S, Mayr E and Klose Z 2013a Glacier and runoff changes in the Rukhk catchment, upper Amu-Darya basin until 2050 *Glob. Planet. Change* **110A** 62–73

Hagg W, Mayer C, Lambrecht A, Kriegel D and Azizov E 2013b Glacier changes in the Big Naryn basin, Central Tian Shan *Glob. Planet. Change* **110A** 40–50

Hamon W R 1961 Estimating potential evapotranspiration *J. Hydraulics Division-ASCE* **87** 107–20

Hawkins E and Sutton R 2009 The potential to narrow uncertainty in regional climate predictions *BAMS* **90** 1095–107

Helsel D R and Hirsch R M 1992 *Statistical Methods in Water Resources* (New York: Elsevier)

Huss M and Farinotti D 2012 Distributed ice thickness and volume of all glaciers around the globe *J. Geophys. Res.* **117** F04010

Huss M, Farinotti D, Bauder A and Funk M 2008 Modelling runoff from highly glacierized alpine drainage basins in a changing climate *Hydrol. Process.* **22** 3888–902

Huss M, Funk M and Ohmura A 2009 Strong Alpine glacier melt in the 1940s due to enhanced solar radiation *Geophys. Res. Lett.* **36** L23501

Huss M, Jouvet G, Farinotti D and Bauder A 2010 Future high-mountain hydrology: a new parameterization of glacier retreat *Hydrol. Earth Syst. Sci.* **14** 815–29

Huss M, Zemp M, Joerg P C and Salzmann N 2014 High uncertainty in 21st century runoff projections from glacierized basins *J. Hydrol.* **510** 35–48

Immerzeel W W, Pellicciotti F and Bierkens M F P 2013 Rising river flows throughout the twenty-first century in two Himalayan glacierized watersheds *Nature Geosci.* **6** 742–5

Jarvis A, Reuter H I, Nelson A and Guevara E 2008 *Hole-Filled Seamless SRTM Data v4*, International Centre for Tropical Agriculture (CIAT), available from http://srtm.csi.cgiar.org (Montpellier, France: CGIAR Consort. for Spatial Inf)

Katchaganov S 2011 *Geomorphology and Palegeography of the Chon Kemin Basin in the Quaternary (in Russian)* (Bishkek: Institute of Geology, National Academy of Science of the Kyrgyz Republic)

Kendall M G 1975 *Rank Correlation Measures* (London: Charles Griffin)

Kirgizgidromet 1936–2002 *National Water Inventory* (Bishkek: Kirgizgidromet)

Kotlyakov V M and Severskiy I V 2009 Glaciers of Central Asia: current situation, changes and possible impact on water resources *Assessment of Snow, Glacier and Water Resources in Asia* **8** 160–77

Kriegel D, Mayer C, Hagg W, Vorogushyn S, Duethmann D, Gafurov A and Farinotti D 2013 Changes in glacierisation, climate and runoff in the second half of the 20th century in the Naryn basin, Central Asia *Glob. Planet. Change* **110A** 51–61

Lutz A F, Immerzeel W W, Gobiet A, Pellicciotti F and Bierkens M F P 2013 Comparison of climate change signals in CMIP3 and CMIP5 multi-model ensembles and implications for Central Asian glaciers *Hydrol. Earth Syst. Sci.* **17** 3661–77

Lutz A F, Immerzeel W W, Shrestha A B and Bierkens M F P 2014 Consistent increase in high Asia's runoff due to increasing glacier melt and precipitation *Nature Clim. Change* **4** 587–92

Mamatkanov D M, Bazhanova L V and Romanovskij V V 2006 *Water Resources of Kyrgyzstan (in Russian)* (Bishkek: Institute of Water Problems and Hydropower, National Academy of Science of the Kyrgyz Republic)

Meinshausen M *et al* 2011 The RCP greenhouse gas concentrations and their extensions from 1765 to 2300 *Clim. Change* **109** 213–41

Oerlemans J 2001 *Glaciers and Climate Change* (Lisse: A.A. Balkema Publishers)

Pellicciotti F, Brock B J, Strasser U, Burlando P, Funk M and Corripio J 2005 An enhanced temperature-index glacier melt model including the shortwave radiation balance: development and testing for Haut Glacier d'Arolla, Switzerland *J. Glaciol.* **51** 573–87

Prudhomme C, Reynard N and Crooks S 2002 Downscaling of global climate models for flood frequency analysis: where are we now? *Hydrol. Process.* **16** 1137–50

Sen P K 1968 Estimates of the regression coefficient based on Kendall's tau *J. Am. Stat. Assoc.* **63** 1379–89

Sorg A, Bolch T, Stoffel M, Solomina O N and Beniston M 2012 Climate change impacts on glaciers and runoff in Tien Shan (Central Asia) *Nature Clim. Change* **2** 725–31

Sorg A, Mosello B, Shalpykova G, Allan A, Hill M and Stoffel M 2014 Coping with changing water resources: the case of the Syr Darya river basin in Central Asia *Environ. Sci. Policy* **43** 68–77

Soviet Topographic Map 1988 *Chok-Tal, K-43-46 1:100 000* (Kyrgyzstan: Bishkek)

Taylor K E, Stouffer R J and Meehl G A 2012 An overview of CMIP5 and the experiment design *BAMS* **93** 485–98

Unger-Shayesteh K, Vorogushyn S, Farinotti D, Gafurov A, Duethmann D, Mandychev A and Merz B 2013 What do we know about past changes in the water cycle of Central Asian headwaters? A review *Glob. Planet. Change* **110A** 4–25

Vilesov E N and Uvarov V N 2001 *Evolution of the Recent Glaciation in the Zailyskiy Alatau in the 20th Century (in Russian)* (Almaty: Kazakh State University)

Vuuren D *et al* 2011 The representative concentration pathways: an overview *Clim. Change* **109** 5–31

WGMS Haeberli W, Gärtner-Roer I, Hoelzle M, Paul F and Zemp M (ed) 2009 *Glacier Mass Balance Bulletin No. 10 (2006-07)* (Zurich: ICSU (WDS)/IUGG (IACS)/UNEP/UNESCO/WMO, World Glacier Monitoring Service) p 96

Ye B, Yang D, Jiao K, Han T, Jin Z, Yang H and Li Z 2005 The urumqi river source glacier no. 1, Tianshan, China: changes over the past 45 years *Geophys. Res. Lett.* **32** L21504

Zhang X, Vincent L A, Hogg W D and Niitsoo A 2000 Temperature and precipitation trends in Canada during the 20th century *Atmos.-Ocean* **38** 395–429

Zhang Y, Liu S and Ding Y 2007 Glacier meltwater and runoff modelling, Keqicar Baqi glacier, southwestern Tien Shan, China *J. Glaciol.* **53** 91–8

The days of plenty might soon be over in glacierized Central Asian catchments

Supplementary Information

Annina Sorg*[1,2], Matthias Huss[3] Mario Rohrer[4] and Markus Stoffel[1,2]

[1] Institute for Environmental Sciences (ISE), University of Geneva, Route de Drize 7, 1227 Carouge, Switzerland

[2] dendrolab.ch, Institute of Geological Sciences, University of Berne, Baltzerstrasse 1+3, 3000 Bern, Switzerland

[3] Department of Geosciences, University of Fribourg, 1700 Fribourg, Switzerland

[4] Meteodat GmbH, Technoparkstrasse 1, 8005 Zurich, Switzerland

1. Data

We used exceptionally long data series of temperature, precipitation, discharge and glacier mass balance to run and calibrate a distributed glacio-hydrological runoff model (Fig. S1).

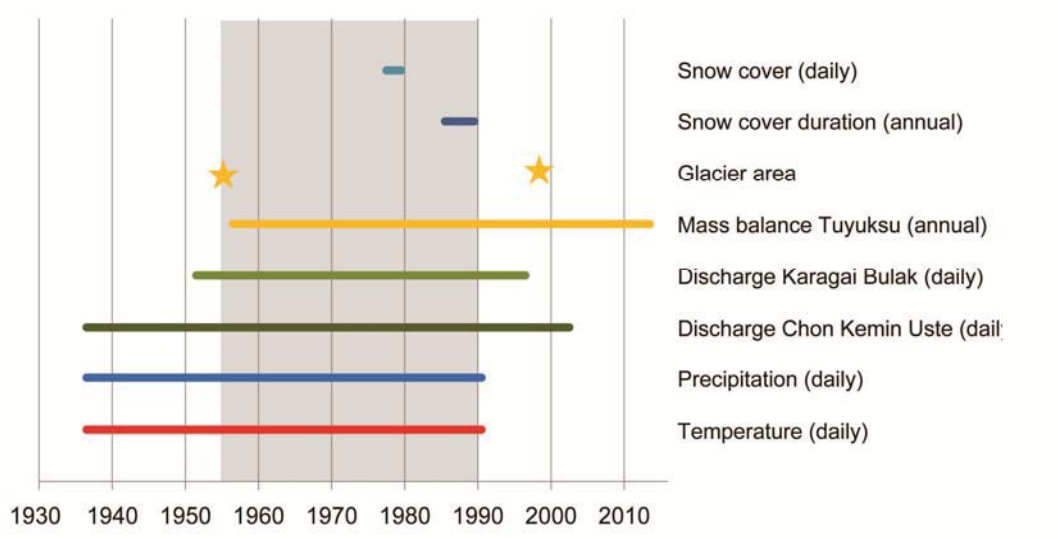

Fig. S1. Data coverage for model input and calibration, with calibration period (1955-1989) displayed in grey.

Temperature and **precipitation** time series from Sabdan station (42.70°N, 76.10°E, 1524 m asl, WMO N° 36921) were available in daily resolution for the time period 1937-1990. The data were downloaded from the Royal Netherlands Meteorological Institute (KNMI) Climate Explorer (http://climexp.knmi.nl).
The precipitation data series contained gaps (02/1955, 1966-1976, 10/1977, 04/1985, 06/1986, 04/07/12/1987), which we filled with daily data from the National Climatic Data Center NOAA (http://www1.ncdc.noaa.gov/pub/data/documentlibrary/tddoc/td9290c.pdf). As the quality of the NOAA data is likely to be lower than the quality of the KNMI data, we have excluded the period 1966-1976 for detailed calibration and used it only to approximate the transient glacier evolution in the past.
As the year 1999 marks the turning point between “past” and “future” in our model, we have extended the measured temperature and precipitation series with downscaled data from the most moderate scenario (dry-cold scenario, see Chapter 4 below) for the period 1990-1999 to allow continuous modeling from 1955 to 2099. The period 1990-1999 is, like 1966-1976, not analyzed in detail.

Discharge data for Chon Kemin Uste (42.67°N, 75.91°E, 1289 m asl) and Karagai Bulak (42.80°N, 76.41°E, 2078 m asl) gauges were available in daily resolution for the time periods 1936-2002 and 1951-1996, respectively. The data were provided by the Kyrgyz National Hydrometeorological Agency (Kirgizgidromet, 1936-2002) and digitized by the authors of this study.

Mass balance and **equilibrium line altitude (ELA)** have been assessed since 1957 at Tuyuksu glacier, which makes them the longest series in Central Asia. We have received the data from the (WGMS Haeberli *et al.*, 2009), the original author is P. A. Cherkasov.

Glacier outlines are from (Bolch, 2007), who mapped the glacier coverage in the Chon Kemin and surrounding valleys using a snow-free Landsat ETM+ scene from 08/08/1999. A TM4/TM5 ratio image was used to delineate the glaciers and misclassified pixels of vegetated areas and lakes were eliminated using the Normalized Difference Vegetation Index (NDVI). We have also digitized glacier outlines reflecting the situation in the 1950s based on topographic maps (Soviet Topographic Map, 1988) to calibrate the model.

Landuse classification for the three non-glacier surface types classified in GERM (forest, vegetation and bare surfaces) has been derived from a supervised classification in Erdas Imagine 8.4 of the same Landsat ETM+ scene as used for the glacier outlines.

Daily snow cover has been used for visual comparison from four Landsat scenes in 1977 (17/04, 23/05, 07/09 and 01/11) and two Landsat scenes in 1979 (30/03 and 12/05). All Landsat scenes were downloaded from http://earthexplorer.usgs.gov/.

Annual snow cover duration has been assessed from the Advanced Very High Resolution Radiometer (AVHRR) at a resolution of 1 km starting in 1986 (Dietz *et al.*, 2013). The data were provided by Andreas Dietz.

The digital elevation model (DEM) and **catchment area delineation** are based on data from the Shuttle Radar Topography Mission SRTM3 (Jarvis *et al.*, 2008). The DEM was resampled from 90 meters to the model resolution of 200 meters. From the SRTM3 DEM, the catchment outline has been derived with ArcGIS Hydrotools. SRTM data were downloaded from http://srtm.csi.cgiar.org/SELECTION/inputCoord.asp.

2. Statistical trend analysis (Mann-Kendall trend test)

Trends in temperature, precipitation and runoff were analyzed with the 2-sided non-parametric Mann-Kendall trend test at the 80, 90 and 95% significance levels (Kendall, 1975; Helsel and Hirsch, 1992). Serial correlation was removed using Sen's slope method (Sen, 1968) and Xuebin Zhang's pre-whitening approach (Zhang *et al.*, 2000). With the help of moving time windows, the multiple trend tests were computed for all time windows of at least 30 years in length during the common 1937-1990 period. The trend matrices in Fig. S2 show the resulting trends (standardized test statistic Z_{MK}; tau) and significance levels (2-sided *p*-value) for key climate variables.

Next 2 pages:
Fig. S2. Summary of the Mann-Kendall (MK) trend test statistics. Trend significance is indicated by the 2-sided p-value and trends are indicated with the standardized test statistics tau.

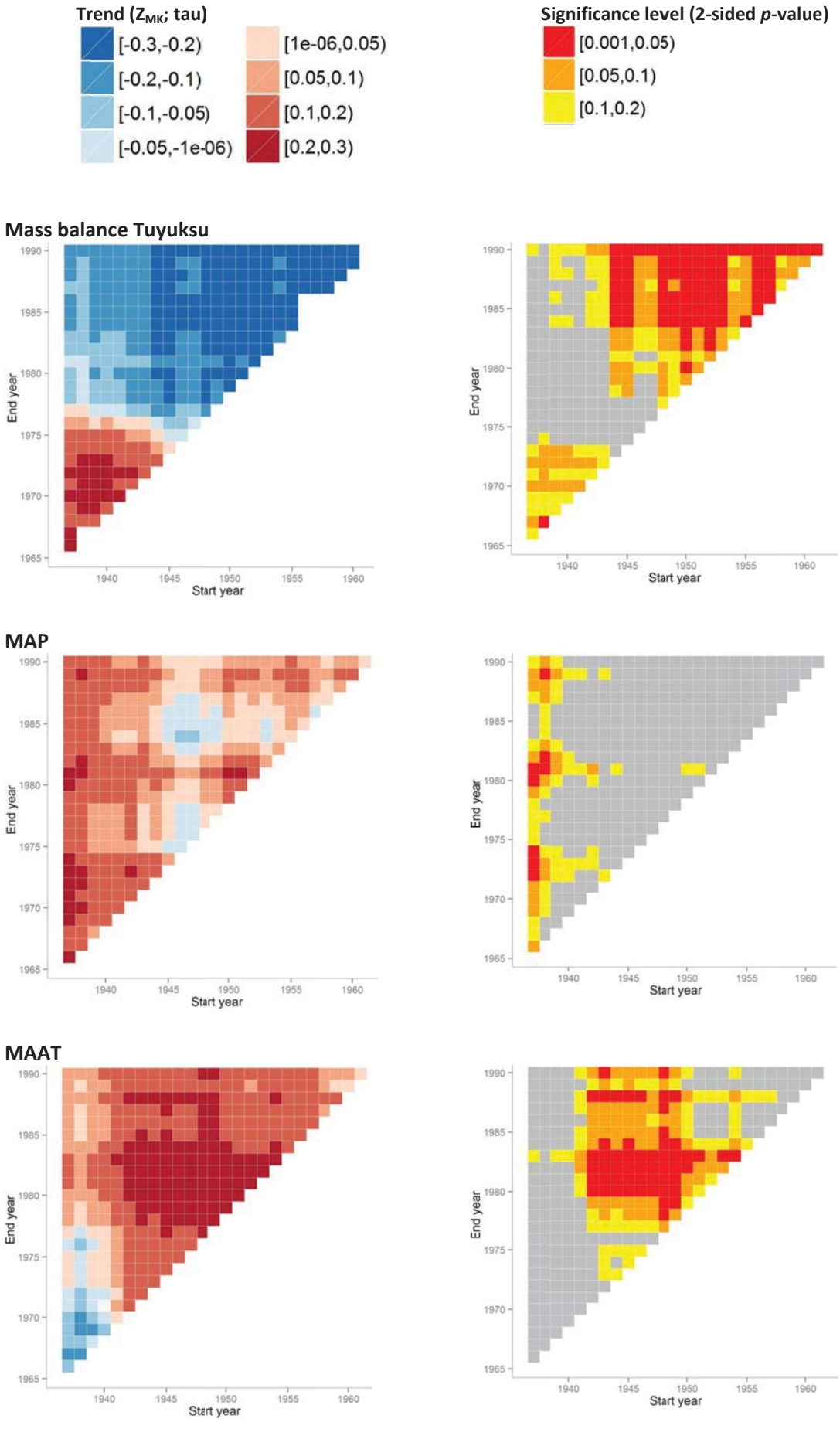
Trend (Z_{MK}; tau)
[-0.3,-0.2)
[-0.2,-0.1)
[-0.1,-0.05)
[-0.05,-1e-06)
[1e-06,0.05)
[0.05,0.1)
[0.1,0.2)
[0.2,0.3)
Significance level (2-sided *p*-value)
[0.001,0.05)
[0.05,0.1)
[0.1,0.2)
Mass balance Tuyuksu
MAP
MAAT
End year
Start year
1965
1970
1975
1980
1985
1990
1940
1945
1950
1955
1960

Summer temperature (JJA)

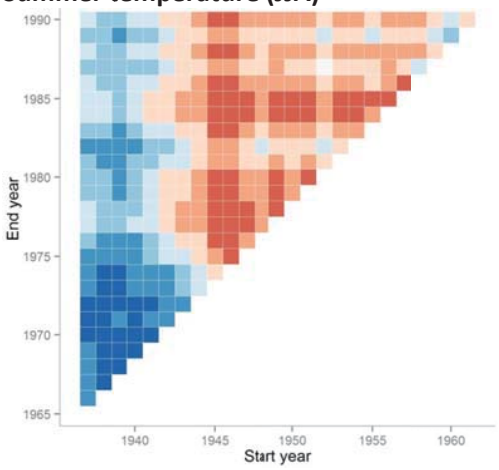

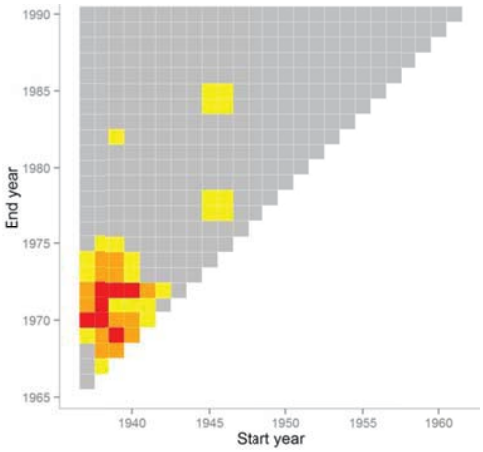

Total runoff Uste

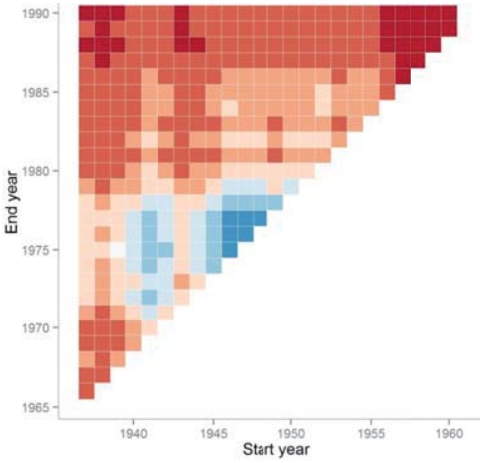

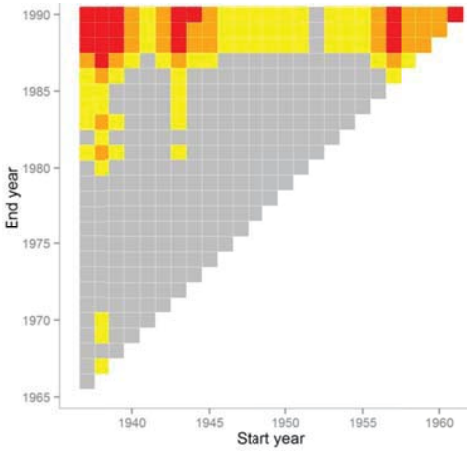

Summer runoff Uste (JJA)

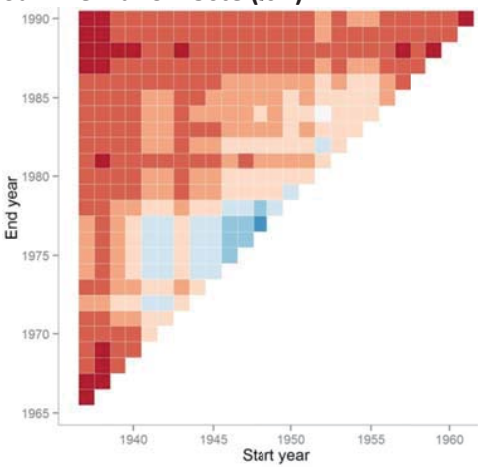

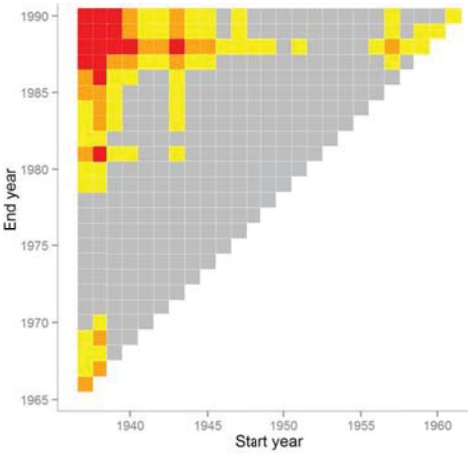

3. Climate data generation

We evaluated all available Global Circulation Model (GCM) runs for the two most extreme representative concentration pathways scenarios (Meinshausen *et al.*, 2011), RCPs 2.6 and 8.5, generated under the Climate Model Intercomparison Project CMIP5 (Taylor *et al.*, 2012) to cover the whole range of possible climatic changes (Vuuren *et al.*, 2011). Under the RCP 2.6 scenario, greenhouse gas emissions and emissions of air pollutants are reduced substantially over time. RCP 8.5 is characterized by increasing greenhouse gas emissions over time representative of scenarios leading to high greenhouse gas concentration levels. All GCM data were downloaded from http://cmip-pcmdi.llnl.gov/cmip5 (01/09/2013).

Downscaling of large-scale GCM output to a finer spatial resolution can be done either with dynamical or statistical approaches (Fowler *et al.*, 2007). Whereas dynamical downscaling requires a higher resolution regional climate model (RCM) to be embedded within a GCM, statistical downscaling establishes empirical relationships between GCM-resolution climate variables and local climate.

We used the statistical "perturbation method" or "delta-change approach" (Prudhomme *et al.*, 2002; Huss *et al.*, 2008b; Smith and Pitts, 1997), thus applying differences between the control and future GCM simulations to baseline observations by adding (temperature) or scaling (precipitation) the mean climatic change to each day. Following the method described in Huss *et al.* (2008b), we use the daily variability of measured time series at Sabdan station and adapt their monthly means along the linear trend line between the standard WMO baseline period (1961-1990) and our future reference period (2081-2099). Using this technique, we obtain meteorological time series with the same resolution, characteristics and variance as in the past.

We then compared all RCP 2.6 and 8.5 GCM runs regarding changes in summer temperature and annual precipitation (mean 2081-2099 vs. 1961-1990; Fig. S3) and chose the four GCM runs which are closest to the 10^{th} and 90^{th} percentiles (Fig. S3), thus representing the range of dry-cold, dry-warm, wet-cold and wet-warm future climates (Immerzeel *et al.*, 2013; Lutz *et al.*, 2013).

Next page:
Fig. S3. Projected changes in climate at Sabdan station, Chon Kemin valley, according to RCPs 2.6 and 8.5 of the CMIP5 dataset. **a**, Changes in summer temperature and annual precipitation based on all GCM runs for 75-77.5°E and 40-45°N (baseline period 1961-1990 vs future period 2081-2099). The range between the 10^{th} and 90^{th} percentiles is shaded in grey. The four GCM runs closest to the percentiles have been chosen for runoff modeling. **b** and **c**, Time series of annual precipitation and summer temperature anomalies for Sabdan meteorological station relative to the 1961-1990 baseline period. The four scenarios represent the range of dry-cold, dry-warm, wet-cold and wet-warm future climates as displayed in Fig. 3a.

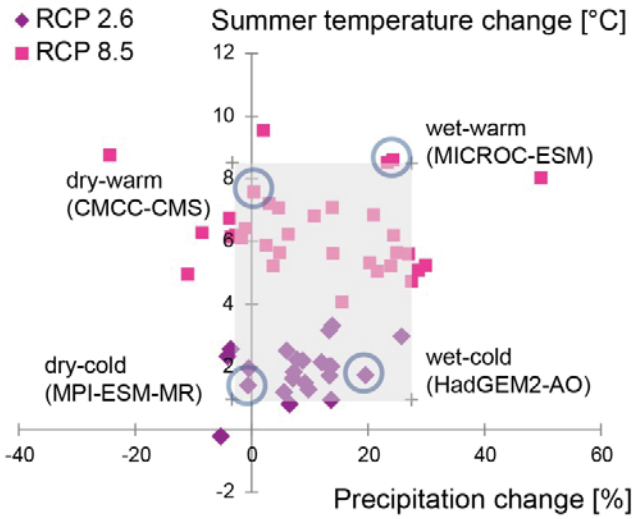
RCP 2.6
RCP 8.5
Summer temperature change [°C]
12
10
8
6
4
2
-2
wet-warm
(MICROC-ESM)
dry-warm
(CMCC-CMS)
dry-cold
(MPI-ESM-MR)
wet-cold
(HadGEM2-AO)
-40
-20
0
20
40
60
Precipitation change [%]

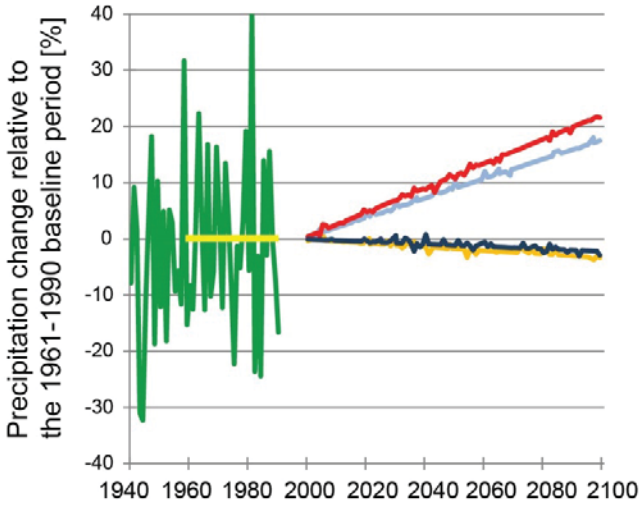
Precipitation change relative to the 1961-1990 baseline period [%]
40
30
20
10
0
-10
-20
-30
-40
1940
1960
1980
2000
2020
2040
2060
2080
2100

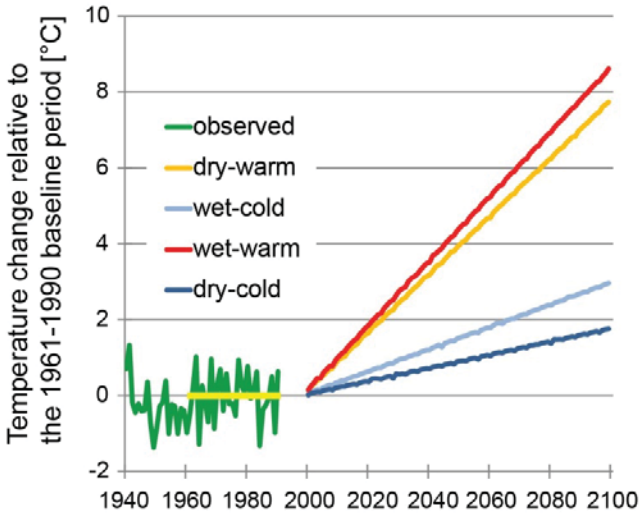
Temperature change relative to the 1961-1990 baseline period [°C]
10
8
6
4
2
0
-2
observed
dry-warm
wet-cold
wet-warm
dry-cold
1940
1960
1980
2000
2020
2040
2060
2080
2100

4. Glacier Evolution Runoff Model GERM

4.1 Calibration and validation procedure

Table S1. Multi-variable calibration of GERM developed for this study.

Parameter group	Criteria	Selection
Climate	Precipitation (4000 m asl)	values from Aizen et al. 2007 ± 10%
	Mean annual evaporation	
	Mean annual runoff	observed ± 10%
Melt	Daily snow cover	visual
	Annual snow cover	observed ± 10%
	Mass balance and ELA	
	Glacier area change	
Routing	Monthly runoff	NS > 0.8

Table S2. Key model parameters of GERM.

Description	Parameter	Value	Unit	Source / Calibrated
Climate parameters				
Precipitation gradient	dP/dz	4.3	%/100m	Bolch (2007)
Temperature gradient	dT/dz	-0.51	°C/100m	Bolch (2007)
Threshold snow / rain	T_{thres}	1.5	°C	Calibrated (range -1-2.5°C)
Actual / potential evaporation	F_{ET}	70-100	%	Calibrated
Snowdrift onto glacier	SD_{gl}	2	-	Calibrated
Melt parameters				
Physical parameter	C_0	-50	W m^{-2}	Calibrated
Physical parameter	C_1	10	W m^{-2} K^{-1}	Oerlemans (2001)
Albedo Ice	α_{ice}	0.35	-	Calibrated (range 0.3-0.5)
Albedo Firn	α_{firn}	0.55	-	Calibrated (range 0.5-0.6)
Albedo Snow	α_{snow}	0.75	-	Calibrated (range 0.7-0.9)
Routing parameters				
Retention slow reservoir	r_{slow}	350	days	Calibrated
Retention ice & firn	r_{ice}	15	days	Calibrated
Retention snow	r_{snow}	20	days	Calibrated
Retention rock	r_{rock}	25	days	Calibrated
Retention pasture	$r_{low\_vegetation}$	40	days	Calibrated
Retention forest	r_{forest}	55	days	Calibrated

Climate parameters

Precipitation was interpolated along a gradient of +4.3% per 100 meters, which corresponds to 31 mm per 100 meters as calculated by Bolch (2007). This gradient is in the range of other studies in the region (Katchaganov, 2011; Hagg *et al.*, 2007). Precipitation was assumed to increase gradually until the crestlines (Katchaganov, 2011; Aizen *et al.*, 1995). This results in interpolated precipitation of 934 mm a^{-1} at 4000 m above sea level, which corresponds well with the results of Aizen et al. (2007; ~950 mm a^{-1}). A threshold of 1.5°C with a linear transition range of ±1°C has been applied to distinguish between solid and liquid precipitation (Ye *et al.*, 2013). Similar to Kuhn (2003), we redistributed a constant fraction of snow fall (SD_{gl} = 2) within the basin from ice-free areas to areas covered by glaciers, as wind and avalanches tend to erode snow from ridges and steep slopes and deposit it in valleys and cirques (Machguth *et al.*, 2006). This snowdrift leads to additional glacier accumulation and to reduced melting as a result of higher albedo for snow than ice.

Temperature was interpolated from Sabdan meteorological station using a gradient of -0.51% per 100 meters (Bolch 2007). This gradient is in the range of other studies in the region (Aizen *et al.*, 1995, 1996; Hagg *et al.*, 2013).

While potential evaporation can be much higher in arid Central Asia than in humid climates, actual evaporation is limited by the low water availability during dry summers (Hagg *et al.*, 2013). An empirical evaporation model is implemented in GERM, which calculates daily potential evaporation based on air temperature and the saturation vapor pressure (Huss *et al.*, 2008b; Hamon, 1961). The model considers five surface types (snow, ice, rock, low vegetation and forest) and has an interception reservoir. Potential evaporation is reduced to actual evaporation for each surface type using a factor F_{ET} that includes a function accounting for soil moisture. The parameters of the evaporation model are calibrated with the values given by Aizen et al. (2007) for the Chon Kemin valley. Modeled mean actual evaporation in the past (1955-1989) is 384 mm, which is in line with previous studies (Aizen *et al.*, 2007; Kuzmichenok, 2008).

Melt parameters

Two melt models are implemented in GERM: an enhanced temperature-index melt model (Hock, 1999; Huss *et al.*, 2008a) and a simplified energy balance equation for net surface energy flux (Oerlemans, 2001; Huss *et al.*, 2008b). The latter approach is less sensitive to temperature changes (Oerlemans, 2001; Pellicciotti *et al.*, 2005), which renders it particularly adequate for modeling in arid regions like Central Asia and over long time periods with significant temperature increases. In the energy balance equation below, the first parenthetical expression represents the shortwave radiation balance and the second parenthetical expression represents long-wave radiation balance and turbulent exchanges:

$$\psi = \{ a\,(1-\alpha)\,Q_E \} + \{ c_0 + c_1 T \}$$

ψ	daily mean surface energy flux (energy available for melting)
a	atmospheric transmission to solar irradiance (reduced incoming shortwave radiation due to cloudiness or haze)
α	surface albedo for snow, ice and firn
Q_E	clear-sky shortwave radiation (mean daily potential global radiation calculated from slope, aspect and topographic shading)
c_0	parameter for turbulent heat exchange
c_1	parameter for longwave radiation balance (10 W m^{-2}, Oerlemans 2001)

Parameter c_1 was set to 10 W m^{-2} K^{-1} and c_0 was used as a tuning parameter (Oerlemans, 2001; Machguth *et al.*, 2006; Painter *et al.*, 2013). Albedo had to be constrained for ice, firn and snow within the respective range of physical characteristics (Paterson, 1994).

Routing parameters

The water available for runoff is determined daily at every grid cell by solving the water balance using the calculated quantities for liquid precipitation, melt and evaporation (Huss *et al.*, 2008b). The runoff routing model is based on the concept of linear storage, with an interception-, slow- and fast reservoir (Farinotti *et al.*, 2012; Huss *et al.*, 2008b). Liquid precipitation first enters the interception reservoir. When the surface-type dependent capacity is exceeded, it is routed into the slow reservoir, which represents subsurface runoff components. The water volume added to the slow reservoir depends on the filling level and on the maximum capacity of the slow reservoir (Schaefli *et al.*, 2005). When the maximum capacity of the slow reservoir is reached, water is routed into the fast reservoir, which represents direct and near-surface runoff components. All reservoirs are emptied at a reservoir-dependent retention constant.

4.2 Calibration and validation results

Annual discharge is well reproduced by the model (Fig. S4). Monthly simulated and observed discharge reach a Nash-Sutcliffe model efficiency coefficient of E = 0.96 (Nash and Sutcliffe, 1970), as shown in Fig. S5.

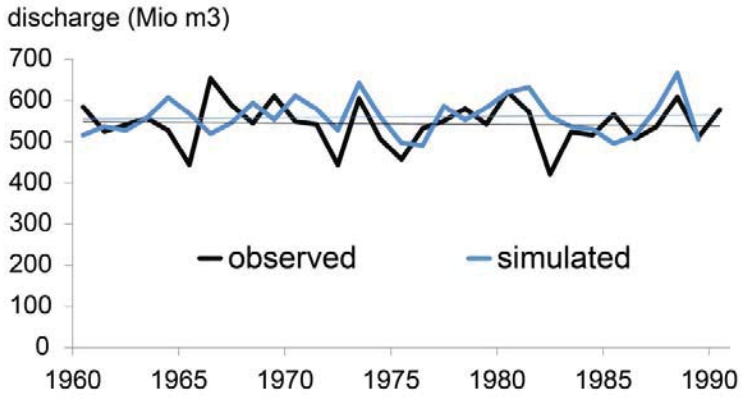

Fig. S4. Simulated and observed annual runoff at Karagai Bulak gauge (1959-1989).

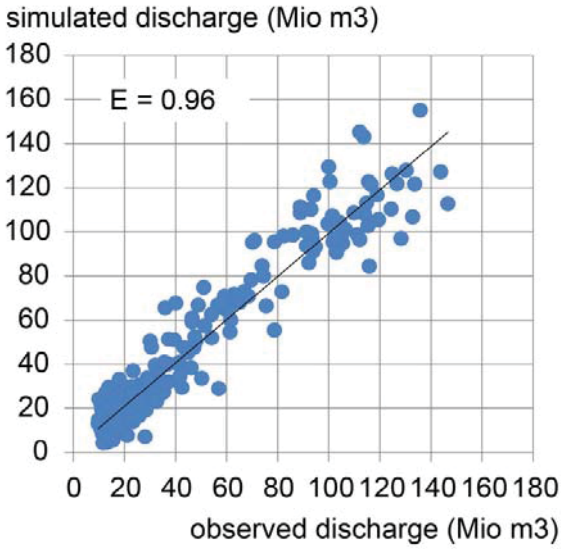

Fig. S5. Simulated and observed monthly runoff at Karagai Bulak gauge (1959-1989, with 1966-1977 excluded due to low quality of meteorological data).
The Nash-Sutcliffe model efficiency criterion E is 0.96 (Nash and Sutcliffe, 1970).

Simulated daily snow cover also corresponds well to visible snow cover on six selected Landsat scenes in 1977 and 1979 (Fig. S6); seasonal accumulation and melting of snow are thus reproduced realistically by the model. Simulated snow cover is displayed with a threshold of 15 mm snow water equivalents, which corresponds to 50 mm snow depth at a snow density of 300

kg m^{-3}. The accumulation season at Tuyuksu Glacier typically starts at the end of August or beginning of September (21/08-22/09) and stops in middle June (02/06-24/06), which is well reproduced by the model (Dyurgerov *et al.*, 1995; Aizen *et al.*, 1996; Schulz, 1965).

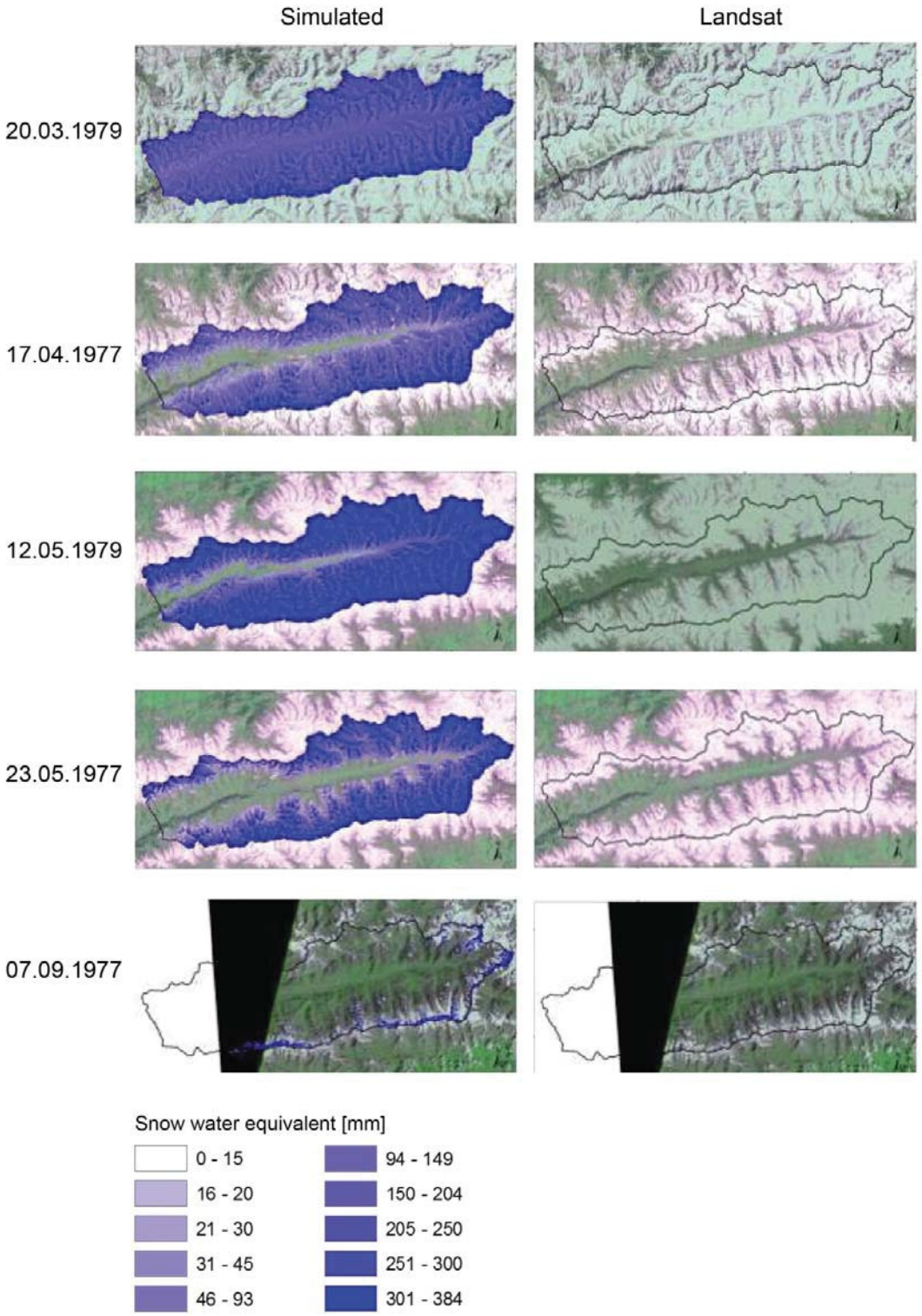

Fig. S6. Simulated and observed snow cover on six randomly chosen days in 1977 and 1979.

Annual snow cover duration is simulated within a 10% range of observed values from AVHRR satellite image analysis (Table S3); snow-rich and snow-poor years are thus well distinguished and the altitudinal snow distribution is well reproduced by the model. Days with more than 91 mm simulated snow water equivalents have been counted for snow cover duration. This higher threshold for AVHRR satellite images as compared to Landsat satellite images is due to the different resolution of AVHRR images (1 km) and Landsat images (30 m). Altitudinal patterns are well represented by the model and years with long snow cover duration (e.g. 1986) are well distinguished from years with shorter snow cover duration (e.g. 1987). Simulated mean annual snow cover duration was always in the range of the observed value ± 10%, except in 1989, when snow cover duration was slightly overestimated.

Table S3. Simulated and observed annual snow cover duration in the Chon Kemin valley (1985-1989).

	Snow cover duration [days]		
Year	**Observed mean**	**Observed ± 10%**	**Simulated mean**
1985	186	168-205	189
1986	218	196-240	206
1987	166	149-182	181
1988	181	163-199	181
1989	179	161-197	149

Simulated glacier surface mass balance and equilibrium line altitude (ELA) in the Chon Kemin valley show the same fluctuations at comparable levels as the series measured at Tuyuksu Glacier (Fig. S7). Simulated average ELA is 3875 m above sea level and thus corresponds to the previously assessed 3900 m above sea level in the Chon Kemin valley (Dyurgerov *et al.*, 1995). As a result of exposure to the North and the higher precipitation rate at Tuyuksu Glacier, ELA is slightly higher in the Chon Kemin valley than at Tuyuksu.

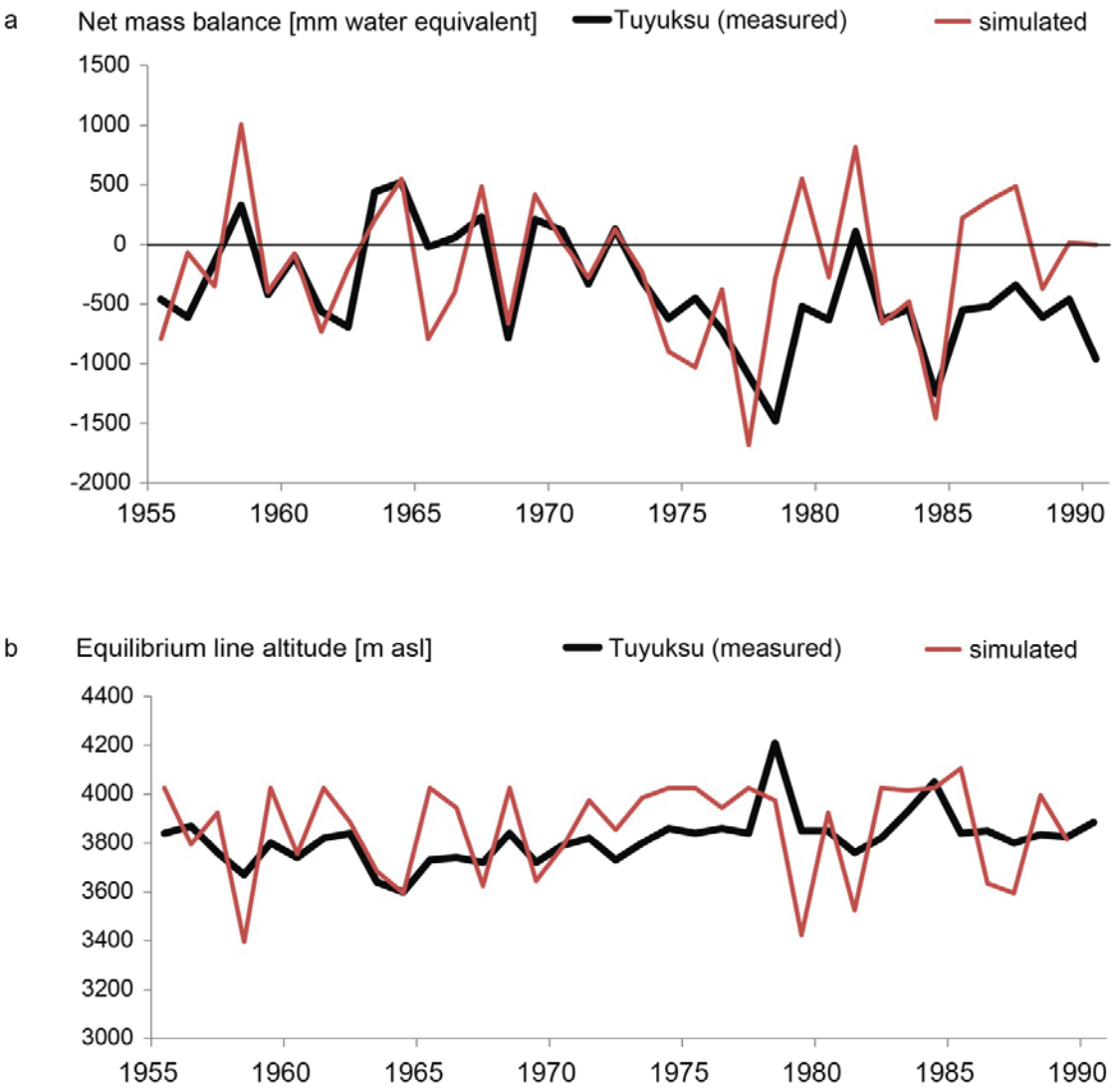

Fig. S7. Simulated and observed mass balance and equilibrium line altitude (ELA) between 1955 and 1990 in the Chon Kemin valley (simulated) and at Tuyuksu Glacier (measured).

The parameterization of glacier retreat is validated by comparing simulated with observed glacier shrinkage rates. The previously assessed annual shrinkage rate of 0.36% a^{-1} for the period 1955-1999 (Bolch, 2007) is reproduced exactly by the model.

References

Aizen V B, Aizen E M and Kuzmichenok V A 2007 Geo-informational simulation of possible changes in Central Asian water resources *Glob. Planet. Change* **56** 341-58

Aizen V B, Aizen E M and Melack J M 1995 Climate, snow cover, glaciers and runoff in the Tien Shan, Central Asia *Journal of the American Water Resources Association* **31** 1113-29

Aizen V B, Aizen E M and Melack J M 1996 Precipitation, melt and runoff in the northern Tien Shan *J Hydrol* **186** 229-51

Bolch T 2007 Climate change and glacier retreat in northern Tien Shan (Kazakhstan/Kyrgyzstan) using remote sensing data *Glob. Planet. Change* **56** 1-12

Dietz A, Kuenzer C, Conrad C and Dech S 2013 Changes of Snow Cover Characteristics in Central Asia between 1986 and 2012 derived from AVHRR and MODIS time series *Eastern Snow Conference*, Huntsville, Ontario, Canada

Dyurgerov M B, Liu C and Zichu X 1995 *Glaciers of Tien Shan (in Russian)* (Moscow: Publishing House VINITI)

Farinotti D, Usselmann S, Huss M, Bauder A and Funk M 2012 Runoff evolution in the Swiss Alps: projections for selected high-alpine catchments based on ENSEMBLES scenarios *Hydrol Process* **26** 1909-24

Fowler H J, Blenkinsop S and Tebaldi C 2007 Linking climate change modelling to impacts studies: recent advances in downscaling techniques for hydrological modelling *Int J Clim* **27** 1547-78

Hagg W, Braun L N, Kuhn M and Nesgaard T I 2007 Modelling of hydrological response to climate change in glacierized Central Asian catchments *J Hydrol* **332** 40-53

Hagg W, Hoelzle M, Wagner S, Mayr E and Klose Z 2013 Glacier and runoff changes in the Rukhk catchment, upper Amu-Darya basin until 2050 *Glob. Planet. Change* **110A** 62-73

Hamon W R 1961 Estimating potential evapotranspiration. *Journal of the Hydraulics Division-ASCE* **87** 107-20

Helsel D R and Hirsch R M 1992 *Statistical methods in water resources* (New York, USA: Elsevier)

Hock R 1999 A distributed temperature-index ice- and snowmelt model including potential direct solar radiation *J Glaciol* **45** 101-11

Huss M, Bauder A, Funk M and Hock R 2008a Determination of the seasonal mass balance of four Alpine glaciers since 1865 *J. Geophys. Res.* **113**

Huss M, Farinotti D, Bauder A and Funk M 2008b Modelling runoff from highly glacierized alpine drainage basins in a changing climate *Hydrol Process* **22** 3888-902

Immerzeel W W, Pellicciotti F and Bierkens M F P 2013 Rising river flows throughout the twenty-first century in two Himalayan glacierized watersheds *Nature Geosci* **6** 742-5

Jarvis J, H. , Reuter A N and Guevara E 2008 *Hole-filled SRTM for the globe, CGIAR-CSI SRTM 90 m Database, Version 4* (Montpellier, France: CGIAR Consort. for Spatial Inf)

Katchaganov S 2011 *Geomorphology and palegeography of the Chon Kemin basin in the Quaternary (in Russian)* (Bishkek: Institute of Geology, National Academy of Science of the Kyrgyz Republic)

Kendall M G 1975 *Rank correlation measures* (London: Charles Griffin)

Kirgizgidromet 1936-2002 *National Water Inventory* (Bishkek: Kirgizgidromet)

Kuhn M 2003 Redistribution of snow and glacier mass balance from a hydrometeorological model *J Hydrol* **282** 95-103

Kuzmichenok V A 2008 *Digital models of moisture characteristics in Kyrgyzstan (in Russian)* (Bishkek: Kyrgyz-Russian University)

Lutz A F, Immerzeel W W, Gobiet A, Pellicciotti F and Bierkens M F P 2013 Comparison of climate change signals in CMIP3 and CMIP5 multi-model ensembles and implications for Central Asian glaciers *Hydrol. Earth Syst. Sci.* **17** 3661-77

Machguth H, Paul F, Hoelzle M and Haeberli W 2006 Distributed glacier mass-balance modelling as an important component of modern multi-level glacier monitoring *Ann Glaciol* **43** 335-43

Meinshausen M, Smith S J, Calvin K, Daniel J S, Kainuma M L T, Lamarque J F, Matsumoto K, Montzka S A, Raper S C B, Riahi K, Thomson A, Velders G J M and Vuuren D P P 2011 The RCP greenhouse gas concentrations and their extensions from 1765 to 2300 *Clim Change* **109** 213-41

Nash J and Sutcliffe J 1970 River flow forecasting through conceptual models part I - A discussion of principles *J Hydrol* **10** 282-90

Oerlemans J 2001 *Glaciers and Climate Change* (Lisse: A.A. Balkema Publishers)

Painter T H, Flanner M G, Kaser G, Marzeion B, VanCuren R A and Abdalati W 2013 End of the Little Ice Age in the Alps forced by industrial black carbon *PNAS*

Paterson W S B 1994 *The physics of glaciers* (Oxford: Pergamon Press)

Pellicciotti F, Brock B J, Strasser U, Burlando P, Funk M and Corripio J 2005 An enhanced temperature-index glacier melt model including the shortwave radiation balance: development and testing for Haut Glacier d'Arolla, Switzerland. *J Glaciol* **51** 573-87

Prudhomme C, Reynard N and Crooks S 2002 Downscaling of global climate models for flood frequency analysis: where are we now? *Hydrol Process* **16** 1137-50

Schaefli B, Hingray B, Niggli M and Musy A 2005 A conceptual glaciohydrological model for high mountainous catchments *Hydrol. Earth Syst. Sci.* **9** 95-109

Schulz V L 1965 *Rivers of Central Asia (in Russian)* (Leningrad: Hydrometeoizdat)

Sen P K 1968 Estimates of the regression coefficient based on Kendall's tau *Journal of the American Statistical Association* **63** 1379-89

Smith J and Pitts G 1997 Regional climate change scenarios for vulnerability and adaptation assessments *Clim Change* **36** 3-21

Soviet Topographic Map 1988 *Chok-Tal, K-43-46 1:100'000* (Bishkek, Kyrgyzstan)

Taylor K E, Stouffer R J and Meehl G A 2012 An overview of CMIP5 and the experiment design *BAMS* **93** 485-98

Vuuren D, Edmonds J, Kainuma M, Riahi K, Thomson A, Hibbard K, Hurtt G, Kram T, Krey V, Lamarque J-F, Masui T, Meinshausen M, Nakicenovic N, Smith S and Rose S 2011 The representative concentration pathways: an overview *Clim Change* **109** 5-31

WGMS Haeberli W, Gärtner-Roer I, Hoelzle M, Paul F and Zemp M (ed) 2009 *Glacier Mass Balance Bulletin No. 10 (2006-07)* (Zurich: ICSU (WDS) / IUGG (IACS) / UNEP / UNESCO / WMO, World Glacier Monitoring Service) p 96

Ye H, Cohen J and Rawlins M 2013 Discrimination of solid from liquid precipitation over northern eurasia using surface atmospheric conditions *J Hydrometeorol* **14** 1345–55

Zhang X, Vincent L A, Hogg W D and Niitsoo A 2000 Temperature and precipitation trends in Canada during the 20th century *Atmosphere-Ocean* **38** 395-429